JOC The Journal of Organic Chemistry

Article

pubs.acs.org/joc

Synthesis and Electron Spin Relaxation of Tetracarboxylate Pyrroline Nitroxides

Shengdian Huang,[†,∥] Joseph T. Paletta,[†,∥] Hanan Elajaili,[‡] Kirby Huber,[‡] Maren Pink,[§] Suchada Rajca,[†] Gareth R. Eaton,[‡] Sandra S. Eaton,*[,‡] and Andrzej Rajca*[,†]

[†]Department of Chemistry, University of Nebraska, Lincoln, Nebraska 68588-0304, United States

[‡]Department of Chemistry and Biochemistry, University of Denver, Denver, Colorado 80208-2436, United States

[§]IUMSC, Department of Chemistry, Indiana University, Bloomington, Indiana 47405-7102, United States

Supporting Information

ABSTRACT: We report the design, synthesis, and electron spin relaxation properties of hydrophilic tetracarboxylate ester pyrroline nitroxides **1** and **2**, which serve as models in the search for new spin labels for DEER distance measurement at room temperature. The nitroxides are designed to have the methyl groups further away from the N−O spin site to decrease the inequivalent couplings of the unpaired electron to the methyl protons that shorten T_m at $T >$ 70 K in currently used labels. The key step in the synthesis of **1** and **2** is the reaction of the dianion of pyrrole-1,2,5-tricarboxylic acid *tert*-butyl ester dimethyl ester with electrophiles such as methyl chloroformate and methyl bromoacetate. Structures of **1** and **2** are confirmed by X-ray crystallography. Studies of electron spin relaxation rates in rigid trehalose/sucrose matrices reveal approximately temperature independent values of $1/T_m$ for **1** and **2** up to about 160 K and modest temperature dependence up to 295 K, demonstrating that increasing the distance between the nitroxide moiety and methyl groups is effective in lengthening T_m at $T >$ 70 K.

INTRODUCTION

Nitroxides are stable organic radicals that have a wide range of applications in chemistry, biochemistry, biophysics, and biomedicine.[1−5] One of the long-standing, remarkable applications is as spin labels, pioneered by McConnell and co-workers in 1965.[6] More recently, the site-directed spin labeling (SDSL) technique coupled with pulsed electron paramagnetic resonance (EPR) dipolar spectroscopy has become one of the techniques of choice for investigating structure and dynamics of biomacromolecules, such as proteins, DNAs, and RNAs.[3,7−19]

Pulsed EPR dipolar spectroscopy, which includes double electron−electron resonance (DEER) and double quantum coherence (DQC), is among the best techniques for accurate measurement of the conformations of flexible regions of biomolecules. Advantages include high sensitivity, a wide range of distances, and absolute distance distributions. The most widely used nitroxide spin label is 1-oxyl-2,2,5,5-tetramethyl-3-pyrroline-3-(methyl)methanethiosulfonate (MTSL) (Figure 1), which selectively binds to cysteine and can be attached at locations introduced by mutagenesis to provide doubly labeled proteins. Relatively small-size nitroxide spin labels typically cause minimal structural perturbation. Among the pulse EPR methods, DEER is the most widely used technique for the measurements of interspin distances of 1.5−8 nm in biomolecules. DEER experiments are typically carried out at temperatures between about 50 and 70 K, requiring use of liquid helium, or with lower sensitivity at 80 K with liquid nitrogen. This restriction to temperatures less than about 80 K is imposed by the rotation of the methyl group in the nitroxide at rates comparable to the inequivalent proton couplings to the unpaired electron. This process shortens the phase memory time, T_m, between about 80 and 300 K.[20,21] T_m is the time constant for the decay of the two-pulse spin echo as the time between pulses is increased. The length of T_m is important because the longer the T_m the stronger the echo at a particular pulse timing, the longer the distance that can be measured, and the more precisely the distribution of distances can be defined.[13,14]

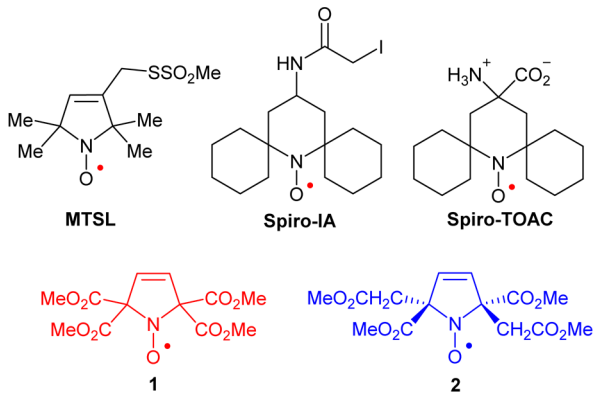

Figure 1. Spin labels and nitroxides **1** and **2**.

Received: November 13, 2016
Published: December 29, 2016

DOI: 10.1021/acs.joc.6b02737
J. Org. Chem. 2017, 82, 1538−1544

We recently prepared a new class of nitroxide spin labels devoid of methyl groups, iodoacetamide (IA) spirocyclohexyl pyrimidine nitroxide, **spiro-IA**, and demonstrated DEER distance measurements at room temperature using T4 Lysozyme (T4L) that was doubly spin labeled with **spiro-IA**. The doubly labeled T4L possesses sufficiently long T_m at Q-band to allow measurement of 4 nm distances at 160 K in glycerol/water and 3 nm distances at room temperature in a trehalose matrix.[22] Replacement of the *gem*-dimethyl groups by conformationally restrained spirocyclohexyl groups diminishes the dynamic averaging effects and lengthens T_m between 80 and 295 K in rigid matrices.[22−25]

The spin labels based on spirocyclohexyl nitroxides are however relatively hydrophobic, which presumably lowers the yield for incorporation of the label at certain sites in proteins, e.g., Cys-8 in T4L.[26] We found that an analogous spirocyclohexyl spin label, i.e., **spiro-TOAC** (as an Fmoc-derivative),[23] could not be efficiently incorporated in phospholamban (PLB).[27]

In the search for a hydrophilic spin label with adequately long T_m for distance measurement at room temperature, we are designing nitroxides with longer T_m compared to the *gem*-dimethyl analogues. Our approach is to decrease the inequivalent couplings of the unpaired electron to the methyl protons that shorten T_m at $T > 70$ K. This can be achieved if the methyl groups are further away from the N−O spin site. Examples of the prototype structure are tetracarboxylate ester pyrroline nitroxides **1** and **2** (Figure 1). Notably, according to the calculated partition coefficients (cLog *P*) and the Connolly solvent excluded volumes (Vol), nitroxides **1** and **2** with four methyl ester groups are much more polar, though somewhat larger, compared to *gem*-dimethyl and spirocyclohexyl analogues (Table 1). Thus, **1** and **2** are excellent models for the novel design of new spin labels.

Table 1. Calculated Partition Coefficients (cLog *P*) and the Connolly Solvent Excluded Volumes (Vol) for Selected Nitroxides[a]

		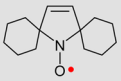	**2**	**1**
cLog *P*	1.16	3.06	0.61	0.78
Vol [Å^3]	149	231	280	250

[a]Geometries of **1** and **2** are optimized at the UB3LYP/6-311G-(d,p)+ZPVE level; see: Tables S5−S7, SI.

Here we report the synthesis of the tetracarboxylate ester pyrroline nitroxides **1** and **2** and their electron spin relaxation rates in rigid trehalose/sucrose matrices.

RESULTS AND DISCUSSION

The synthesis of nitroxides **1** and **2** starts from commercially available *N*-Boc-pyrrole which is then converted to pyrrole **3** in one step according to the procedures for the synthesis of pyrrolizidine alkaloids (Scheme 1, Supporting Information (SI)).[28,29] Subsequently, the dianion of **3** in THF is generated using the conditions reported for preparation of the *cis*-2,5-tetrasubstituted pyrroline, which was formed by quenching the dianion with 2,6-di-*tert*-butylphenol. Because our target is the *trans*-isomer, we quench the dianion of **3** with electrophiles, $ClCO_2Me$ and $BrCH_2CO_2Me$, to provide products **4** and **6**,

Scheme 1. Synthesis of Nitroxides 1 and 2

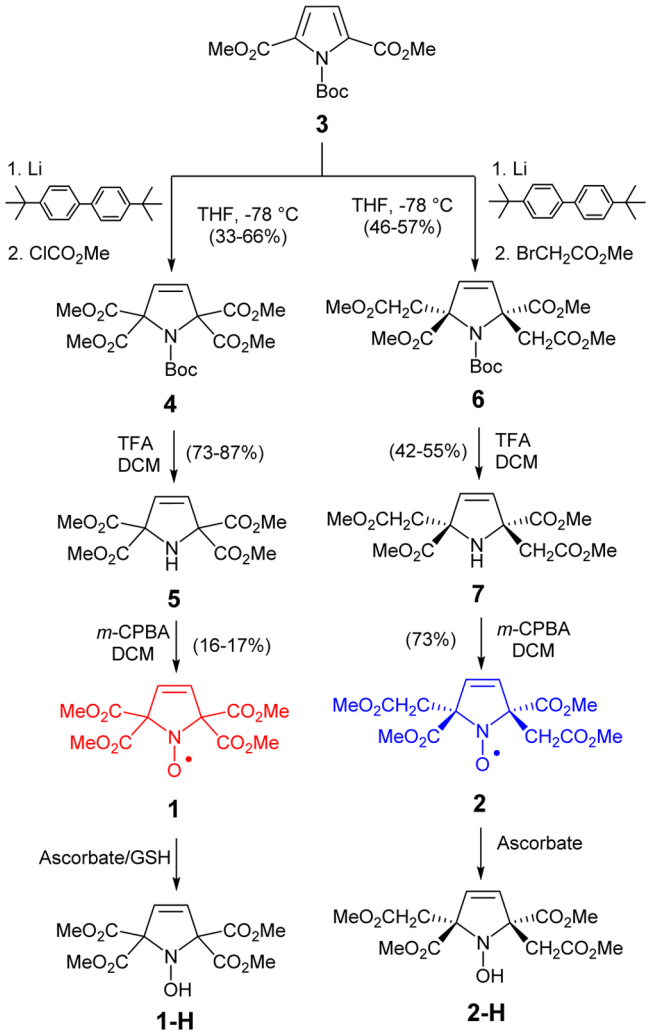

respectively. In analogy to the reported reaction of the dianion of **3** with an acid,[28] we expect a bulky electrophile such as $BrCH_2CO_2Me$ to provide a similar outcome. That is, after the first C−C bond formation, the resulting monoenolate anion reacts, *from the least hindered face*, with the second molecule of $BrCH_2CO_2Me$, to produce *trans*-**6**. Subsequent deprotections of the *N*-Boc groups with trifluoroacetic acid (TFA) in dichloromethane (DCM) provided amines **5** and **7**, which are then oxidized to the corresponding nitroxides **1** and **2**, using *meta*-chloroperbenzoic acid (*m*-CPBA) in DCM.

Structures of nitroxides **1** and **2** are confirmed by single-crystal X-ray analysis (Figure 2). In particular, the *trans*-stereochemistry for **2**, which is C_2-symmetric in the crystal, is unequivocally confirmed.

Purity of nitroxides **1** and **2** was confirmed by paramagnetic ^{1}H NMR spectra and EPR spectroscopic spin concentrations. In addition, nitroxides **1** and **2** are reduced, using an excess of ascorbate and reduced glutathione (GSH), to the corresponding diamagnetic hydroxylamines **1-H** and **2-H**. Lastly, structures of **1-H** and **2-H** are confirmed by ^{1}H and ^{13}C NMR spectroscopy, IR spectroscopy, and mass spectrometry.

EPR spectra of nitroxides **1** and **2** in chloroform show triplet patterns due to isotropic ^{14}N hyperfine coupling with $A(^{14}N)$ = 34.2 and 37.7 MHz, respectively; *g*-values are near 2.006 (Figure 3). For **1**, each of the triplet peaks is resolved into

DOI: 10.1021/acs.joc.6b02737
J. Org. Chem. 2017, 82, 1538−1544

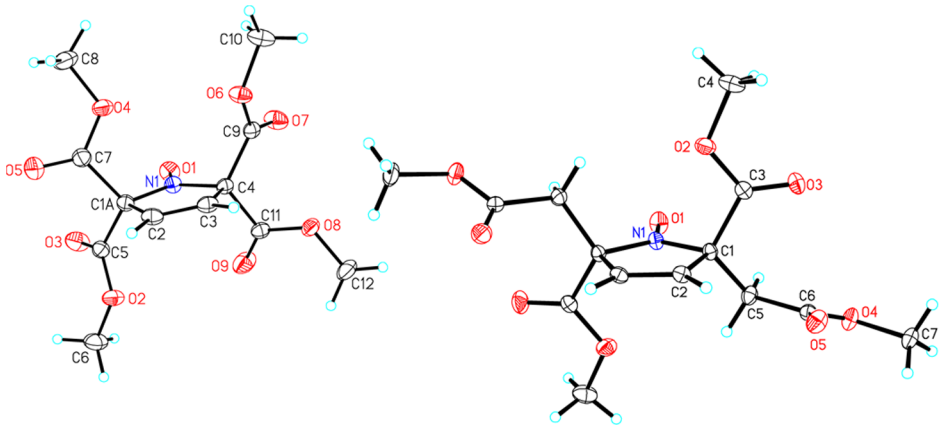

Figure 2. X-ray structures for nitroxide radicals **1** (left) and **2** (right). Carbon, nitrogen, and oxygen atoms are depicted with thermal ellipsoids set at the 50% probability level.

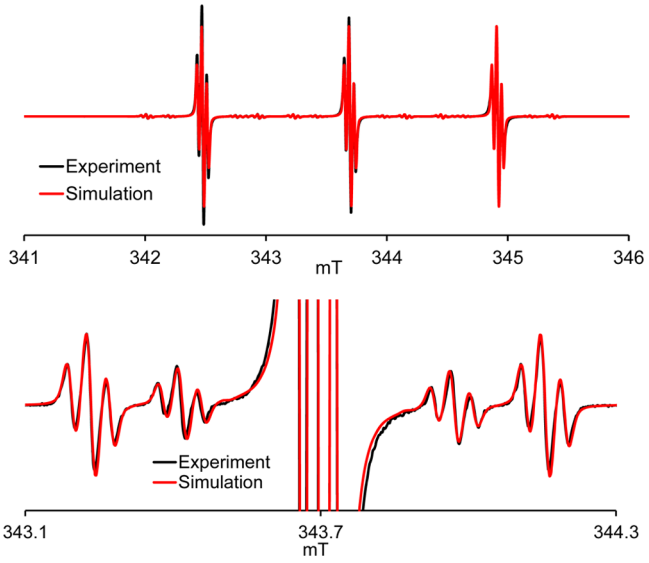

Figure 3. EPR (ν = 9.6505 GHz) spectrum of 0.1 mM nitroxide **1** in chloroform. (Top panel) Complete spectrum; (bottom panel) expansion plot near the center peak showing ^{13}C satellite peaks. Simulation: g = 2.0062, $A(^{14}N)$ = 34.2 MHz (n = 1), $A(^{1}H)$ = 1.10 MHz (n = 2), $A(^{15}N)$ = 48.1 MHz (n = 1), $A(^{13}C)$ = 25.3 MHz (n = 4), $A(^{13}C)$ = 15.5 MHz (n = 2), Lorentzian/Gaussian = 0.4, LW = 0.020 mT (all nuclei are at natural abundance).

triplets, corresponding to the coupling of two vinylic protons with isotropic ^{1}H hyperfine coupling, $A(^{1}H)$ = 1.10 MHz (top panel in Figure 3).

Two well resolved side bands originating from ^{13}C hyperfine couplings of two quaternary carbons and four carbonyl (C═O) carbons with $A(^{13}C)$ = 15.5 and 25.3 MHz, respectively, are observed (bottom panel in Figure 3, Table 2). Similarly, for **2**, multiplet patterns are observed, corresponding to the hyperfine coupling of three pairs of protons, i.e., protons of the vinylic group and diastereotopic protons within the methylene (CH_2) groups, with $A(^{1}H)$ = 1.86, 1.43, and 1.09 MHz (Figure S9, SI).

Notably, the EPR spectral line widths are rather narrow, ≤ 0.02 mT, indicating that the unresolved isotropic hyperfine couplings from protons of the methyl groups are very small, i.e., $A(^{1}H)$ < 0.1 MHz. This finding is confirmed by paramagnetic ^{1}H NMR spectroscopy.[30−32] For **1**, the spectrum consists of a singlet peak at δ = 4.72 ppm and the other, much broader singlet at δ = −22.9 ppm (Figure 4).

Table 2. Experimental and DFT-Computed Isotropic ^{1}H Hyperfine Couplings ($A(^{1}H)$ in MHz) for Nitroxides 1 and 2[a]

	(Me)		(vinylic)			(CH_2)[b]		
	EPR	NMR[c]	EPR[d]	NMR[c]	DFT	EPR[d]	NMR[c]	DFT
1[e]	–	+0.034	1.10	−1.08	−1.68	–	–	–
2	–	+0.058	1.43	−1.26	−1.80	1.09	−1.6	−1.37
		+0.017				1.86		−1.94

[a]DFT computations at the UB3LYP/EPR-III//UB3LYP/6-311G-(d,p)+ZPVE level; because no conformational analysis of the methyl groups was carried out, the computed values of $A(^{1}H)$ for the methyl groups are not reported. [b]Protons in the CH_2 moiety are diastereotopic. [c]For paramagnetic ^{1}H NMR spectra of **1** and **2**, see: Figures S15, S16, S24, and S25, SI. [d]For fluid solution CW EPR spectra of **1** and **2** with spectral simulations, see: Figures S7−S9, SI. [e]Computed values of $A(^{13}C)$ (in MHz) in C_2-symmetric **1** are −16.9 for C1 and C4 (quaternary carbons), +30.5 and +22.2 (avg. = +26.4) for C9−C13 (carbonyl carbons); all other carbons have relatively small values of $A(^{13}C) \leq 0.5$ MHz, and thus their sidebands are not resolved in the experimental spectrum.

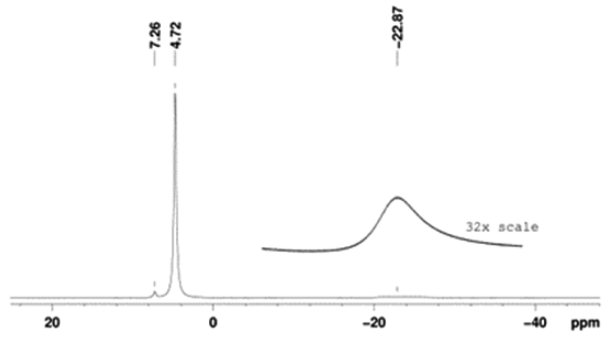

Figure 4. Paramagnetic ^{1}H NMR (400 MHz) spectrum for 0.9 M nitroxide **1** in chloroform-*d*.

Based on the corresponding paramagnetic shifts (vs diamagnetic reference such as **1-H**), the values of isotropic ^{1}H hyperfine couplings are $A(^{1}H)$ = +0.034 MHz and $A(^{1}H)$ = −1.08 MHz for the methyl and vinylic protons, respectively. Similar analyses for **2** (and **2-H**) provide $A(^{1}H)$ = +0.058 MHz and $A(^{1}H)$ = +0.017 MHz for the two types of methyl protons (Table 2).[33] For comparison, an ∼1 order of magnitude larger value of $|A(^{1}H)|$ = 0.90 MHz for the methyl group protons was measured in a typical five-membered ring *gem*-dimethyl

DOI: 10.1021/acs.joc.6b02737
J. Org. Chem. 2017, 82, 1538−1544

nitroxide such as Proxyl.[34] Values of isotropic $A(^{14}N)$ and of the anisotropic $A_{zz}(^{14}N)$ (Figures S5 and S6, SI) increase in the order **1** < **2** < MTSL. The smaller hyperfine couplings for the carboxy-substituted nitroxides are attributed to the electron-withdrawing and electron delocalization effects of the carboxylate groups.[35]

Using the lowest energy C_2-symmetric conformational minima for **1** and **2**, identified at the UB3LYP/6-311G-(d,p)+ZPVE level of theory, the UB3LYP-computed values of isotropic $A(^1H)$ using the EPR-III basis set are in qualitative agreement with experiment (Table 2).[36] For **1**, the computed values of isotropic $A(^{13}C)$ for quaternary and carbonyl carbons well reproduce experimental values (Footnote in Table 2 and Figure 3).

Electron spin relaxation times were measured on samples immobilized in a glassy sugar matrix consisting of 90% trehalose and 10% sucrose. Trehalose has been shown to cryoprotect biomaterials better than other sugars.[37] Trehalose also maintains protein function and enzyme activity better than dehydrated sucrose.[38,39] Glasses containing 10% sucrose were observed to be more stable during drying than 100% trehalose glasses. If the glass crystallizes, the solute is excluded from the lattice which results in locally high concentrations of solute that enhance relaxation rates (Figure S4, SI). The temperature dependence of $1/T_m$ for **1** and **2** at the X- and Q-band is summarized in Figure 5. Rates at both frequencies were

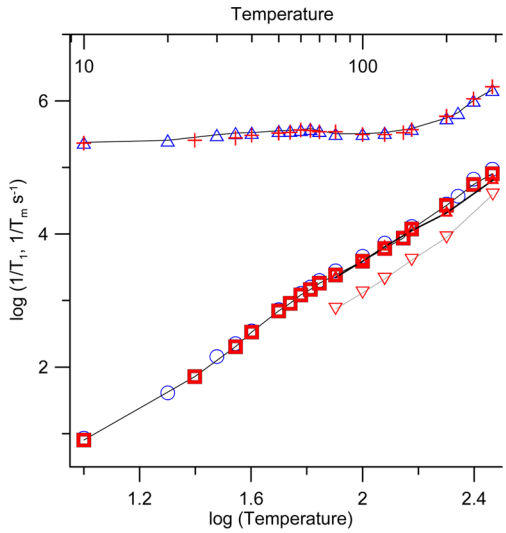

Figure 5. Temperature dependence of $1/T_1$ at X-band (9.44 GHz) in the perpendicular plane (blue circles) **1**, (red squares) **2**, and at Q-band (33.90 GHz) in the perpendicular plane (red triangles) **2**, along the *z*-axis (red inverted triangles) **2**. Temperature dependence of $1/T_m$ at X-band in the perpendicular plane (blue triangles) **1**, (red plus) **2**. Lines connect the data points. Samples were in 9:1 trehalose/sucrose.

measured at the field that corresponds to the maximum amplitude of the absorption spectrum. Relaxation rates are similar for the two radicals. We observe that $1/T_m$ is approximately independent of temperature below about 160 K. Notably, the $1/T_m$ values for **1** and **2** in trehalose/sucrose at T < 160 K are similar to those observed for spirocyclohexyl nitroxides in 1:1 water/glycerol at T < 70 K,[22,23] except that we observe a small enhancement in $1/T_m$ at about 60 to 70 K. We attribute this enhancement to the rotation of the carboxy methyl groups at rates comparable to the electron proton dipolar coupling. This effect on $1/T_m$ is much smaller than in the case of the traditional *gem*-dimethyl groups of MTSL because the electron−proton couplings are much smaller, as suggested by the relatively small values of isotropic $A(^1H)$ (Table 2). It occurs at lower temperatures than those for *gem*-dimethyl groups of MTSL because the barrier to rotation is smaller. This enhancement would be a small disadvantage for DEER experiments at 40 to 70 K but not a factor for experiments at higher temperatures, with optimum conditions, i.e., long T_m and short T_1, at about 120 K. At temperatures above about 160 K, the $1/T_m$ relaxation rates increase, which is attributed to increasing motion of the radicals in the lattice and shorter T_1. The $1/T_m$ values for the two radicals remain similar at the X- and Q-band.

The spin−lattice relaxation rate, $1/T_1$, is important for the DEER experiments because it determines how quickly the signal averaging can be repeated. The temperature dependence of $1/T_1$ for **1** and **2** in the perpendicular plane of the molecule is similar at X- and Q-band and similar for the two radicals (Figure 5). This result is consistent with the expectation that the Raman process dominates spin−lattice relaxation at lower temperatures and a local mode process dominates at higher temperatures.[40] The $1/T_1$ relaxation rates for both of these processes are independent of the microwave frequency. Previous studies demonstrated that $1/T_1$ is slower near the parallel axis of the *g*-matrix (along the p-π orbital of the nitrogen) than in the perpendicular plane.[41] At Q-band, anisotropy is more highly resolved than at X-band, and the anisotropy in $1/T_1$ is readily observed (Figure 5). At temperatures up to about 200 K, $1/T_1$ for these radicals in trehalose/sucrose is similar to values for **Spiro-TOAC** in 1:1 water/glycerol.[23] The water/glycerol glass softens and melts at about 200 K, whereas the trehalose/sucrose glass remains relatively rigid at ambient temperature. In the relatively rigid trehalose/sucrose glass, there is negligible contribution to $1/T_1$ from modulation of *g* and *A*-anisotropy, so relaxation rates at temperatures above about 200 K are slower in this environment than in water/glycerol.[40]

Minimal dependence of $1/T_m$ on the position in the spectrum is important for the DEER experiments, because the amplitude of the echo that is used to monitor the electron−electron dipolar interaction depends on T_m. If T_m were much shorter for some orientations of the molecule in the magnetic field than for others, those orientations would be under-represented in the DEER response. Orientation dependence of $1/T_m$ was examined in detail at Q-band. Field-swept echo detected spectra of **2** are shown in Figure 6. The spectrum at 80 K is typical for immobilized nitroxides. The amplitude at each position in the spectrum depends on the fraction of radicals on resonance at that field and on the value of $1/T_m$. The extremum of the absorption spectrum at about 1213 mT (position 3 in Figure 6) corresponds to molecules with nitrogen $m_I = -1$ that are aligned with the magnetic field along the molecular *z*-axis. The region of the spectrum near 1212 mT corresponds to molecules with the magnetic field at an orientation that is intermediate between the *z*-axis and the *xy* plane, and is particularly sensitive to motions that alter the orientation of the molecular *z*-axis relative to the external field on the time scale of the spin echo experiment.[42]

At 293 K the decreased amplitude of the field-swept echo-detected signal at about 1212 mT (position 2) relative to that at about 1213 mT (position 3) reflects the increase in $1/T_m$ at the intermediate orientation of the molecule that arises from motion on the time scale of the spin−echo experiment. Values

DOI: 10.1021/acs.joc.6b02737
J. Org. Chem. 2017, 82, 1538−1544

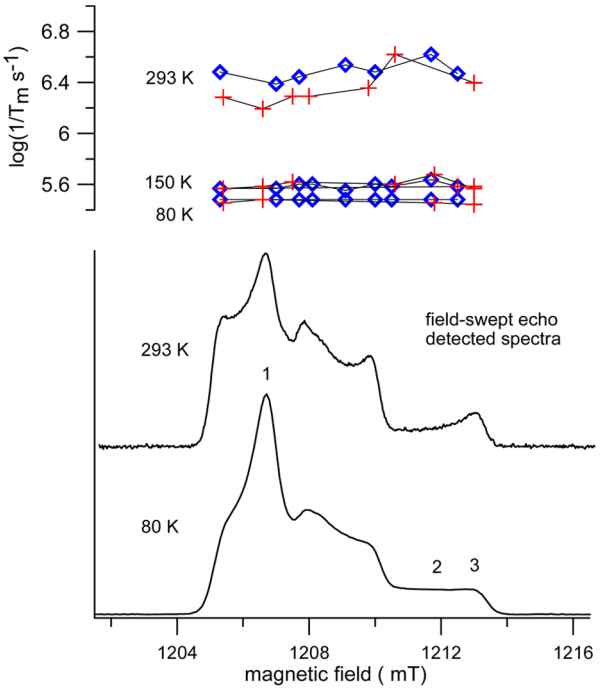

Figure 6. Lower panel: Field-swept echo-detected spectra for **2** in 9:1 trehalose/sucrose at 33.90 GHz at 80 and 293 K. Positions labeled as 1, 2, and 3 correspond, respectively, to resonance for molecules with the magnetic field in the *xy* plane, an orientation intermediate between the *z*-axis and the *xy* plane, and near the *z*-axis. The upper panel displays $1/T_m$ as a function of position in the spectrum for **1** (blue diamonds) and **2** (red plus) at 80, 150, and 293 K.

of $1/T_m$ for **1** and **2** as a function of position in the spectrum are shown in the upper panel of Figure 6. Between 80 and 150 K there is little temperature dependence of $1/T_m$, and values show little dependence on position in the spectrum, as is expected when the radical is well immobilized. Relaxation rates at 293 K are faster than at lower temperature and more dependent on position in the spectrum. The slowest rates are observed at position 1, which is in the perpendicular plane. At this position in the spectrum, low amplitude motions cause little change in resonance field.[42] The fastest relaxation rates are near position 2, where the resonance field is more sensitive to motion. However, even at 293 K, the variation of $1/T_m$ through the spectrum of **1** or **2** is less than a factor of 2.5 for the positions at which values were recorded.

Electron spin relaxation rates at room temperature for nitroxides immobilized in trehalose matrices have been compared for nitroxides with a range of structures.[25] The concern was expressed that structures and substituents that made T_m longer also made T_1 longer. The signal-to-noise in the DEER experiment is much more strongly dependent on T_m than on T_1. The intensity of an echo at a particular time between pulses depends exponentially on T_m. Thus, a factor of 2 decrease in T_m, decreases the echo intensity by a factor of e^{-2} = 0.14, which means that the echo is only 14% of what it would have been at the longer T_m. A factor of 2 increase in T_1 only increases the data acquisition time by a factor of 2. Furthermore, near room temperature T_1 of nitroxides is short enough that the duty cycle of the high power amplifiers may limit the pulse repetition time, rather than the nitroxide relaxation. Thus, modest increases in T_1 that accompany lengthening of T_m are not a major concern. It is also expected that rigid attachment of a spin label to a macromolecule will enhance immobilization and lengthen T_m beyond what is observed for the small molecule nitroxides.

CONCLUSION

The approximately temperature independent value of $1/T_m$ for **1** and **2** up to about 160 K and modest temperature dependence up to 295 K demonstrate that increasing the distance between the nitroxide moiety and methyl groups is effective in increasing T_m at $T > 70$ K. Rigid attachment to a biomolecule is expected to further limit motion at room temperature and thereby decrease $1/T_m$ and the orientation dependence of $1/T_m$.

EXPERIMENTAL SECTION

Synthesis of 1 and 2. Chemicals and per-deuterated solvents for NMR spectroscopy were obtained from commercial sources and used as received unless otherwise indicated. Purification and titration of commercial *m*-CPBA (70%) were carried out as previously described.[43] 1-(*tert*-Butyl)-2,5-dimethyl 1*H*-pyrrole-1,2,5-tricarboxylate (**3**) was prepared according to the literature method.[28,29] Column chromatography was carried out on flash grade silica gel, using 0−20 psig pressure. Preparative TLC (PTLC) was carried out using tapered silica plates with a preadsorbent zone.

NMR spectra were obtained using commercial spectrometers (^{1}H, 300, 400, and 700 MHz) using chloroform-*d* ($CDCl_3$) as solvent. The 700 MHz instrument was equipped with a cryoprobe. The chemical shift references were as follows: (^{1}H) chloroform, 7.260 ppm and (^{13}C) chloroform-*d*, 77.2 ppm. Typical 1D FID was subjected to exponential multiplication with an exponent of 0.3 Hz (^{1}H) or 1 Hz (^{13}C). IR spectra were obtained using a commercial instrument, equipped with an ATR sampling accessory. MS analyses were carried out at the local mass spectrometry facility.

Detailed procedures for all new compounds may be found in the SI.

*1-(tert-butyl)-2,2,5,5-Tetramethyl-1H-pyrrole-1,2,2,5,5-pentacarboxylate (**4**) and 1-(tert-Butyl)-2,5-dimethyl-trans-2,5-bis(2-methoxy-2-oxoethyl)-2,5-dihydro-1H-pyrrole-1,2,5-tricarboxylate (**6**).* 4,4′-Di-*tert*-butylbiphenyl (1 equiv) in THF was added to Li metal (20+ equiv) in THF at 0 °C. After stirring for 3 h, the reaction mixture was cooled to −78 °C and a solution of **3** (2 equiv) in THF (0.2−0.4 mM) was added dropwise.[28] After 16 h, the dark brown liquid part of the reaction mixture (i.e., dianion of **3**) was cannulated to mostly frozen methyl chloroformate (2 equiv) or methyl bromoacetate (2 equiv) and then stirred for 1 d at −78 °C. After addition of saturated aqueous ammonium chloride the reaction mixture was allowed to reach room temperature. Subsequent aqueous workup with diethyl ether provided crude products, which were purified by column chromatography (silica gel, pentane/ethyl acetate, 1:1): **4**, R_f 0.32, 1.86 g (66%) from 2.0 g of **3**, and for **6**, R_f 0.52, 0.71 g (47%) from 1.0 g of **3**. In the ^{1}H and ^{13}C NMR spectra of **4** and **6**, some of the peaks are doubled due to the presence of two conformers of the Boc group.[28,29] Characterization for compound **4**. Light yellow solid, mp 105−107 °C. ^{1}H NMR (700 MHz, $CDCl_3$): δ 6.139 (d, J = 5.9 Hz, 1H), 6.108 (d, J = 5.9 Hz, 1H), 3.816 (s, 6H), 3.811 (s, 6H), 1.440 (s, 9H). ^{13}C NMR (100 MHz, $CDCl_3$): δ 166.8, 151.8, 130.5, 130.1, 82.4, 78.85, 78.75, 53.4, 53.2, 28.1. HRMS (ESI/TOF-Q) m/z: $[M + Na]^+$ calcd for $C_{17}H_{23}NO_{10}Na$ 424.1220; found 424.1216. IR (diamond, cm^{-1}): 3101, 2996, 2976, 2957, 1772, 1746, 1717, 1433, 1368, 1231, 1203, 1166, 1131, 1091, 1045, 1012, 970, 906, 845, 810, 766, 738, 719, 624. Characterization for compound **6**. Light yellow oil. ^{1}H NMR (300 MHz, $CDCl_3$): δ 6.43 (d, J = 6 Hz, 1H), 6.40 (d, J = 6 Hz, 1H), 3.723 (s, 6H), 3.690 (s, 6H), 3.71 (d, $J \approx$ 10 Hz, 1H), 3.490 (d, J = 15 Hz, 1H), 2.910 (dd, J = 15 Hz, J = 6.0 Hz, 2H), 1.432 (s, 9H). ^{13}C NMR (75 MHz, $CDCl_3$): δ 170.89, 170.75, 170.60, 170.54, 151.5, 131.7, 131.5, 82.3, 74.4, 73.7, 53.2, 53.1, 51.90, 51.80, 40.7, 39.4, 28.3. HRMS (ESI/TOF-Q) m/z: $[M + Na]^+$ calcd for $C_{19}H_{27}NO_{10}Na$ 452.1533; found 452.1543. IR (diamond, cm^{-1}): 2984, 2954, 1738, 1703, 1436,

DOI: 10.1021/acs.joc.6b02737
J. Org. Chem. 2017, 82, 1538−1544

1349, 1329, 1289, 1220, 1160, 1110, 1068, 1001, 899, 864, 845, 801, 771, 716, 670.

*Tetramethyl-1H-pyrrole-2,2,5,5-tetracarboxylate (**5**) and Dimethyl-trans-2,5-bis(2-methoxy-2-oxoethyl)-2,5-dihydro-1H-pyrrole-2,5-dicarboxylate (**7**).* To compound **4** (2.64 g, 6.57 mmol, 1 equiv) or **6** (0.400 g, 0.932 mmol, 1 equiv) in dichloromethane (DCM, 0.02−0.1 mM) trifluoroacetic acid (TFA, 30−300 equiv) was added at 0 °C. Following the addition, the reaction mixture was kept for 5 min at 0 °C, and then it was stirred at room temperature for 1−2 h, until TLC analyses indicated the absence of the starting material. DCM and TFA were rapidly removed under vacuo; the resultant crude product was treated with methanol (3 times), which was then removed under vacuo. Purification by column chromatography (silica gel) gave the products: compound **5**, methanol/DCM, 3:97, R_f 0.48, 1.720 g (87%); compound **7**, pentane/ethyl acetate, 3:1, R_f 0.15, 0.127 g (42%). Characterization of compound **5**. Sand colored solid, mp 46−52 °C. ^{1}H NMR (600 MHz, $CDCl_3$): δ 6.156 (s, 2H), 3.801 (s, 12H). ^{13}C NMR (176 MHz, $CDCl_3$): δ 169.4, 130.5, 79.4, 53.5. HRMS (ESI/TOF-Q) m/z: $[M + Na]^+$ calcd for $C_{12}H_{15}NO_8Na$ 324.0695; found 324.0685. IR (diamond, cm^{-1}): 3318, 3011, 2958, 2844, 1735, 1435, 1267, 1226, 1153, 1073, 1034, 965, 928, 860, 804, 765, 734, 699. Characterization for compound **7**. Brown solid, mp 80−81 °C. ^{1}H NMR (300 MHz, $CDCl_3$): δ 5.908 (s, 2H), 3.688 (d, J = 18 Hz, 12H), 2.929 (d, J = 16 Hz, 4H). ^{13}C NMR (75 MHz, $CDCl_3$): δ 173.9, 171.2, 132.7, 73.9, 53.0, 52.0, 43.7. HRMS (ESI/TOF-Q) m/z: $[M + H]^+$ Calcd for $C_{14}H_{20}NO_8$ 330.1189; Found 330.1177. IR (diamond, cm^{-1}): 3398, 3091, 2957, 1731, 1713, 1433, 1410, 1354, 1320, 1285, 1274, 1244, 1202, 1174, 1079, 1059, 1047, 994, 890, 850, 808, 797, 758, 708.

*Nitroxides **1** and **2**.* 0.1−0.4 mM purified *m*-CPBA[43] (3.8 equiv) in DCM was added dropwise to 0.3−0.4 mM **5** (0.849 g, 2.82 mmol) or **7** (250 mg, 0.76 mmol) in DCM in an ice bath (0 °C). Following the addition, the resultant mixture was stirred for 5 min at 0 °C, and then for 2−3 h at room temperature. The solvents were removed under vacuum, and the residue was dissolved in diethyl ether, washed with aqueous saturated sodium bicarbonate and brine, dried over sodium sulfate, filtered, and evaporated, to provide a crude product. The crude was purified with column chromatography (silica gel, chloroform/ethyl acetate, 2:1, R_f 0.45) and then treated with diethyl ether to provide nitroxide **1** (145 mg, 16%) or purified by column chromatography (silica gel, pentane/ethyl acetate, 3:1, R_f = 0.31) to provide nitroxide **2** (190 mg, 73%). Characterization of nitroxide **1**. Orange powder, mp 127−129 °C. EPR (X-band, 0.1 mM in C_6H_6): spin concentration 99%. Paramagnetic ^{1}H NMR (400 MHz, $CDCl_3$): δ 4.72 (s), −22.87 (bs). HRMS (ESI/TOF-Q) m/z: $[M + Na]^+$ calcd for $C_{12}H_{14}NO_9Na$ 339.0566; found 339.0578. IR (diamond, cm^{-1}): 3121, 2961, 1759, 1737, 1441, 1340, 1244, 1168, 1115, 1047, 960, 918, 890, 801, 769, 728, 659, 640. Characterization for nitroxide **2**. Light yellow solid, mp 119−120 °C. EPR (X-band, 0.1 mM in chloroform): spin concentration ∼100%. Paramagnetic ^{1}H NMR (400 MHz, $CDCl_3$): δ 5.31 (s), 4.13 (s), −27.72 (bs), −40 (very bs). HRMS (ESI/TOF-Q) m/z: $[M + Na]^+$ calcd for $C_{14}H_{18}NO_9Na$ 367.0879; found 367.0870. IR (diamond, cm^{-1}): 2965, 2916, 2848, 2160, 1978, 1745, 1725, 1432, 1414, 1359, 1336, 1267, 1226, 1209, 1169, 1128, 1062, 1003, 977, 965, 922, 901, 853, 797, 766, 716, 674, 626.

*Hydroxylamines: Tetramethyl-1-hydroxy-1H-pyrrole-2,2,5,5-tetracarboxylate (**1-H**) and Dimethyl-trans-1-hydroxy-2,5-bis(2-methoxy-2-oxoethyl)-2,5-dihydro-1H-pyrrole-2,5-dicarboxylate (**2-H**).* Nitroxide **1** (5.1 mg) or nitroxide **2** (10.6 mg) was dissolved in a pH 7.4 buffered ascorbate solution: for **1**, 2 mL, 20 mM ascorbate, 20 mM reduced glutathione, and 125 mM phosphate; for **2**, 2.5 mL, 0.062 mM ascorbate, 12.4 mM phosphate. For **1** and **2**, the reaction mixtures were stirred at room temperature under the exclusion of light for 15 min and 3 h, respectively. Subsequent extraction with ethyl acetate, drying over sodium sulfate, and removal of solvents provided crude products **1-H** and **2-H**. Characterization for crude **1-H**. ^{1}H NMR (700 MHz, $CDCl_3$): δ 6.605 (bs, 1H), 6.180 (s, 2H), 3.811 (s, 12H). ^{13}C NMR (176 MHz, $CDCl_3$): δ 167.5, 130.3, 82.2, 53.3. HRMS (ESI/TOF-Q) m/z: $[M + Na]^+$ calcd for $C_{12}H_{15}NO_9Na$ 340.0645; found 340.0642. IR (diamond, cm^{-1}): 3440 (br), 2958, 1733, 1434, 1255, 1155, 1039, 801. Characterization for crude **2-H**. ^{1}H NMR (700 MHz, $CDCl_3$): δ 6.105 (s, 2H), 5.79 (bs, 1H), 3.755 (s, 6H), 3.665 (s, 6H), 3.294 (d, J = 17 Hz, 2H), 2.893 (d, J = 17 Hz, 2H). ^{13}C NMR (176 MHz, $CDCl_3$): δ 171.7, 171.3, 131.7, 78.1, 52.8, 51.9, 39.3. HRMS (ESI/TOF-Q) m/z: $[M]^+$ calcd for $C_{14}H_{19}NO_9$ 345.1060; found 345.1069. IR (diamond, cm^{-1}): 3442 (br), 2955, 1733, 1437, 1348, 1207, 1079, 1005, 785.

X-ray Crystallography of 1 and 2. For **1** and **2**, crystals were obtained by slow evaporation of a DCM/heptane (1:1) solution and vapor diffusion of pentane into a chloroform solution, respectively. Data were collected at low temperature using a commercial diffractometer for **1** and synchrotron radiation for **2**. Data reduction and absorption corrections were carried out using standard procedures. Structure solutions were obtained by intrinsic methods.[44] Further details are provided in the SI PDF and CIF files.

Electron Spin Relaxation Studies. Samples for relaxation time measurements were prepared as follows: Solutions of 0.1 mM nitroxide in 1:1 water/ethanol were mixed with an aqueous solution containing 9:1 trehalose/sucrose. The mole ratio of sugars to nitroxide was 2000:1. The solutions were placed in a thin layer on a watch glass. The solvent evaporated overnight, forming a glassy film. The film was scraped off the water glass and transferred to a 4 mm quartz EPR tube. EPR tubes were evacuated on a vacuum line overnight to remove oxygen and residual water and then flame-sealed. Samples for the Q-band were aliquots of materials that had been dried in vacuum overnight and then transferred to 1.8 mm quartz capillaries, without further evacuation.

Relaxation times at the X- and Q-band were measured. T_m was measured by two-pulse echo decay using a $\pi/2 - \tau - \pi - \tau -$ echo sequence and initial τ = 200 or 300 ns. T_1 was measured by inversion recovery using a $\pi - T - \pi/2 - \tau - \pi - \tau -$ echo sequence with a constant τ = 800 ns at Q-band or 600 ns at X-band. The lengths of the $\pi/2$ pulses were 40 ns. The temperature dependence of relaxation was monitored at the field that corresponds to the maximum amplitude in the absorption spectrum. At the X-band this position is near the center of the spectrum, and at the Q-band this position is near the low-field end of the spectrum. At both frequencies these positions correspond predominantly to molecules for which the magnetic field is in the molecular *xy* plane. Echo decays and inversion recovery curves were fitted with single exponentials.

■ ASSOCIATED CONTENT

Supporting Information

The Supporting Information is available free of charge on the ACS Publications website at DOI: 10.1021/acs.joc.6b02737.

Crystallographic data (CIF, CIF)

General procedures and materials, additional experimental details, spectral data, computational data tables, and complete ref 36 (PDF)

■ AUTHOR INFORMATION

Corresponding Authors

*E-mail: arajca1@unl.edu.

*E-mail: sandra.eaton@du.edu.

ORCID

Andrzej Rajca: 0000-0002-8856-1536

Author Contributions

‖S.H. and J.T.P. contributed equally.

Notes

The authors declare no competing financial interest.

■ ACKNOWLEDGMENTS

We thank the National Science Foundation and National Institutes of Health for support of this work through Grants CHE-1362454 (A.R.), NIBIB R01 EB019950-02 (A.R. and

S.S.E.), and NIGMS U54GM087519-06 (A.R.). ChemMatCARS Sector 15 is principally supported by the National Science Foundation/Department of Energy under Grant Number NSF/CHE-1346572. Use of the Advanced Photon Source was supported by the U.S. Department of Energy, Office of Science, Office of Basic Energy Sciences, under Contract No. DE-AC02-06CH11357. We thank Dr. Xinming Liu (UNL) for his help with the synthesis and Dr. Nolan Gallagher (UNL) for his help with the EasySpin spectral simulations.

REFERENCES

(1) Tebben, L.; Studer, A. *Angew. Chem., Int. Ed.* **2011**, *50*, 5034−5068.
(2) Krishna, M. C.; Russo, A.; Mitchell, J. B.; Goldstein, S.; Dafni, H.; Samuni, A. *J. Biol. Chem.* **1996**, *271*, 26026−26031.
(3) Hubbell, W. L.; Lopez, C. J.; Altenbach, C.; Yang, Z. *Curr. Opin. Struct. Biol.* **2013**, *23*, 725−733.
(4) Weaver, J.; Burks, S. R.; Liu, K. J.; Kao, J. P. Y.; Rosen, G. M. *J. Magn. Reson.* **2016**, *271*, 68−74.
(5) (a) Rajca, A.; Wang, Y.; Boska, M.; Paletta, J. T.; Olankitwanit, A.; Swanson, M. A.; Mitchell, D. G.; Eaton, S. S.; Eaton, G. R.; Rajca, S. *J. Am. Chem. Soc.* **2012**, *134*, 15724−15727. (b) Sowers, M. A.; McCombs, J. R.; Wang, Y.; Paletta, J. T.; Morton, S. W.; Dreaden, E. C.; Boska, M. D.; Ottaviani, M. F.; Hammond, P. T.; Rajca, A.; Johnson, J. A. *Nat. Commun.* **2014**, *5*, 5460.
(6) Stone, T. J.; Buckman, T.; Nordio, P. L.; McConnell, H. M. *Proc. Natl. Acad. Sci. U. S. A.* **1965**, *54*, 1010−1017.
(7) Altenbach, C.; Flitsch, S. L.; Khorana, H. G.; Hubbell, W. L. *Biochemistry* **1989**, *28*, 7806−7812.
(8) Altenbach, C.; Marti, T.; Khorana, H. G.; Hubbell, W. L. *Science* **1990**, *248*, 1088−1092.
(9) Jeschke, G.; Sajid, M.; Schulte, M.; Ramezanian, N.; Volkov, A.; Zimmermann, H.; Godt, A. *J. Am. Chem. Soc.* **2010**, *132*, 10107−10117.
(10) Akyuz, N.; Georgieva, E. R.; Zhou, Z.; Stolzenberg, S.; Cuendet, M. A.; Khelashvili, G.; Altman, R. B.; Terry, D. S.; Freed, J. H.; Weinstein, H.; Boudker, O.; Blanchard, S. C. *Nature* **2015**, *518*, 68−73.
(11) Joseph, B.; Sikora, A.; Cafiso, D. S. *J. Am. Chem. Soc.* **2016**, *138*, 1844−1847.
(12) Roser, P.; Schmidt, M. J.; Drescher, M.; Summerer, D. *Org. Biomol. Chem.* **2016**, *14*, 5468−5476.
(13) Jeschke, G. *Annu. Rev. Phys. Chem.* **2012**, *63*, 419−446.
(14) Baber, J. L.; Louis, J. M.; Clore, G. M. *Angew. Chem., Int. Ed.* **2015**, *54*, 5336−5339.
(15) Borbat, P. P.; Mchaourab, H. S.; Freed, J. H. *J. Am. Chem. Soc.* **2002**, *124*, 5304−5353.
(16) Borbat, P. P.; Davis, J. H.; Butcher, S. E.; Freed, J. H. *J. Am. Chem. Soc.* **2004**, *126*, 7746−7747.
(17) Yang, Z. Y.; Liu, Y. P.; Borbat, P.; Zweier, J. L.; Freed, J. H.; Hubbell, W. L. *J. Am. Chem. Soc.* **2012**, *134*, 9950−9952.
(18) Azarkh, M.; Singh, V.; Okle, O.; Seemann, I. T.; Dietrich, D. R.; Hartig, J. S.; Drescher, M. *Nat. Protoc.* **2012**, *8*, 131−147.
(19) Shevelev, G. Y.; Krumkacheva, O. A.; Lomzov, A. A.; Kuzhelev, A. A.; Rogozhnikova, O. Y.; Trukhin, D. V.; Troitskaya, T. I.; Tormyshev, V. M.; Fedin, M. V.; Pyshnyi, D. V.; Bagryanskaya, E. G. *J. Am. Chem. Soc.* **2014**, *136*, 9874−9877.
(20) Dzuba, S. A.; Maryasov, A. G.; Salikhov, K. M.; Tsvetkov, Yu. D. *J. Magn. Reson.* **1984**, *58*, 95−117.
(21) Nakagawa, K.; Candelaria, M. B.; Chik, W.W. C.; Eaton, S. S.; Eaton, G. R. *J. Magn. Reson.* **1992**, *98*, 81−91.
(22) Meyer, V.; Swanson, M. A.; Clouston, L. J.; Boratyński, P. J.; Stein, R. A.; Mchaourab, H. S.; Rajca, A.; Eaton, S. S.; Eaton, G. R. *Biophys. J.* **2015**, *108*, 1213−1219.
(23) Rajca, A.; Kathirvelu, V.; Roy, S. K.; Pink, M.; Rajca, S.; Sarkar, S.; Eaton, S. S.; Eaton, G. R. *Chem. - Eur. J.* **2010**, *16*, 5778−5782.
(24) Kirilyuk, I. A.; Polienko, Y. F.; Krumkacheva, O. A.; Strizhakov, R. K.; Gatilov, Y. V.; Grigor'ev, I. A.; Bagryanskaya, E. G. *J. Org. Chem.* **2012**, *77*, 8016−8027.
(25) Kuzhelev, A. A.; Strizhakov, R. K.; Krumkacheva, O. A.; Polienko, Y. F.; Morozov, D. A.; Shevelev, G. Y.; Pyshnyi, D. V.; Kirilyuk, I. A.; Fedin, M. V.; Bagryanskaya, E. G. *J. Magn. Reson.* **2016**, *266*, 1−7.
(26) Personal communication from Drs. Elka R. Georgieva, Peter P. Borbat, and Jack H. Freed (Cornell University). Approximately 8% efficiency in labelling of Cys-8 in T4L with **Spiro-IA** was determined; the reason for this low efficiency was not established.
(27) Personal communication from Dr. Christine B. Karim (University of Minnesota).
(28) Donohoe, T. J.; Headley, C. E.; Cousins, R. P. C.; Cowley, A. *Org. Lett.* **2003**, *5*, 999−1002.
(29) (a) Donohoe, T. J.; Thomas, R. E.; Cheeseman, M. D.; Rigby, C. L.; Bhalay, G.; Linney, I. D. *Org. Lett.* **2008**, *10*, 3615−3618 (b) NMR data for compound **3** from refs 28 and 29a: ^{1}H NMR (400 MHz, $CDCl_3$) δ 6.84 (2 H, s), 3.87 (6 H, s), 1.67 (9 H, s); ^{13}C NMR (101 MHz, $CDCl_3$) δ 159.9, 148.9, 126.7, 115.8, 86.3, 52.0, 27.3. (c) NMR data for compound **3**: ^{1}H NMR (300 MHz, $CDCl_3$): δ 6.83 (s, 2H), 3.86 (s, 6H), 1.66 (s, 9H). ^{13}C NMR (176 MHz, $CDCl_3$): δ 160.0, 149.0, 126.8, 115.9, 86.4, 52.1, 27.4.
(30) la Mar, G. N., Ed. *Nuclear Magnetic Resonance of Paramagnetic Macromolecules*; Springer: Netherlands, 1995; pp 1 − 391.
(31) Olankitwanit, A.; Kathirvelu, V.; Rajca, S.; Eaton, G. R.; Eaton, S. S.; Rajca, A. *Chem. Commun.* **2011**, *47*, 6443−6445.
(32) Gallagher, N. M.; Bauer, J. J.; Pink, M.; Rajca, S.; Rajca, A. *J. Am. Chem. Soc.* **2016**, *138*, 9377−9380.
(33) These two values of $A(^{1}H)$ = +0.058 and +0.017 MHz in nitroxide **2** are the higher and lower bounds, due to uncertainty in the assignment of the resonances for the methyl groups in **2** and in **2-H**.
(34) (a) Biller, J. R.; Meyer, V.; Elajaili, H.; Rosen, G. M.; Kao, J. P. Y.; Eaton, S. S.; Eaton, G. R. *J. Magn. Reson.* **2011**, *212*, 370−377. (b) Rockenbauer, A.; Gyor, M.; Hankovszky, H. O.; Hideg, K. *Electron Spin Resonance* **1988**, *11*, 145−182.
(35) Rassat, A. *Molecular Spectroscopy*; Institute of Petroleum, distributed by Elsevier Publishing, Brighton, U.K., 1968; pp 145−155.
(36) Frisch, M. J., et al. *Gaussian 09*, Revision A.01; Gaussian, Inc.: Wallingford, CT, 2009.
(37) Crowe, J. H.; Carpenter, J. F.; Crowe, L. M. *Annu. Rev. Physiol.* **1998**, *60*, 73−103.
(38) Martinez, L. M.; Videa, M.; Mederos, F.; deMoral, Y. *J. Mex. Chem. Soc.* **2011**, *55*, 185−189.
(39) Möbius, K.; Savitsky, A.; Nalepa, A.; Malferrari, M.; Francia, F.; Lubitz, W.; Venturoli, G. *Appl. Magn. Reson.* **2015**, *46*, 435−464.
(40) Yu, Z.; Quine, R. W.; Rinard, G. A.; Tseitlin, M.; Elajaili, H.; Kathirvelu, V.; Clouston, L. J.; Boratyński, P. J.; Rajca, A.; Stein, R. A.; Mchaourab, H. S.; Eaton, S. S.; Eaton, G. R. *J. Magn. Reson.* **2014**, *247*, 67−71.
(41) Du, J.-L.; Eaton, G. R.; Eaton, S. S. *J. Magn. Reson., Ser. A* **1995**, *115*, 213−221.
(42) Du, J.-L.; More, K. M.; Eaton, S. S.; Eaton, G. R. *Isr. J. Chem.* **1992**, *32*, 351−355.
(43) Rajca, A.; Shiraishi, K.; Rajca, S. *Chem. Commun.* **2009**, 4372−4374.
(44) Sheldrick, G. M. *Acta Crystallogr., Sect. C: Struct. Chem.* **2015**, *71*, 3−8.

DOI: 10.1021/acs.joc.6b02737
J. Org. Chem. 2017, 82, 1538−1544